

Bachelor's thesis at the Lucerne School of Engineering and Architecture

Title	Crystallization of Phase Change Materials under Space Conditions
Student	Enderli, Julia
Bachelor's degree program	Bachelor in Energy and Environmental Systems Engineering
Semester	fall semester 25
Lecturer	Stamatiou, Anastasia
Industry Partner	CC Thermische Energiespeicher, Hochuli Adina
External examiner	Lieball, Kai

Abstract English

Phase change materials (PCMs) offer high energy density thermal buffering with near-isothermal heat absorption and release, making them attractive for mass- and power-constrained thermal management in space systems. However, crystallization of inorganic salt hydrate PCMs under terrestrial gravity is strongly affected by buoyancy-driven convection and sedimentation, which can promote phase segregation, void formation, and reduced cycling reliability. This Bachelor thesis provides experimental groundwork for a future European Space Agency sounding-rocket (MASER) experiment by characterizing key risks and design inputs for controlled PCM solidification under microgravity-relevant constraints.

A structured decision process compared sodium acetate trihydrate (SAT) and calcium chloride hexahydrate (CCH) and evaluated cooling-power-driven versus supercooling-dominated operation. SAT was selected due to safer handling, predominantly congruent melting, and a pronounced, externally triggerable supercooled state, whereas CCH was excluded because of corrosivity, hygroscopicity, incongruent melting tendencies, and lower controllability. Laboratory testing focused on SAT hydration stability, mechanical robustness, and thermal response. Water content was measured using Karl Fischer titration and a halogen moisture analyzer, revealing a substantial method-dependent discrepancy; Karl Fischer titration was adopted as the reference and samples were adjusted to the standard water content. Mechanical stability of molten SAT was assessed via analytical centrifugation (LumiSizer), showing stable behavior under stepwise increased centrifugal loading without signatures of macroscopic crystallization. Thermal cycling experiments using an EasyMax reactor with heat-flow calorimetry demonstrated that deep cooling to sub-zero temperatures induces supercooling signatures, but temperature control alone did not reliably produce complete crystallization within short cycle durations, indicating the need for an active triggering mechanism and/or extended low-temperature dwell times.

Overall, the results support a supercooling-based experimental strategy with SAT and provide concrete boundary conditions for payload design, including mandatory hydration verification, robustness against launch-relevant mechanical loading, and the requirement for controlled nucleation to ensure crystallization during the microgravity window.

Abstract German

Phasenwechselmaterialien (Phase Change Materials, PCMs) ermöglichen aufgrund ihrer hohen Energiedichte und nahezu isothermen Wärmeaufnahme und -abgabe eine effiziente thermische Pufferung und sind daher besonders für masse- und leistungsbeschränkte thermische Managementsysteme in der Raumfahrt geeignet. Die Kristallisation anorganischer Salzhydrat-PCMs wird unter terrestrischen Schwerkraftbedingungen stark durch auftriebsgetriebene Konvektion und Sedimentation beeinflusst, was Phasensegregation, Hohlraumbildung und eine reduzierte Zyklen Stabilität begünstigt. Diese Bachelorarbeit liefert experimentelle Grundlagen für ein zukünftiges Sounding-Rocket-Experiment der European Space Agency (MASER-Plattform) zur kontrollierten PCM-Erstarrung unter mikrogravitationsrelevanten Randbedingungen.

Ein strukturierter Entscheidungsprozess verglich Natriumacetat-Trihydrat (SAT) und Calciumchlorid-Hexahydrat (CCH) sowie kühlleistungsdominierte und unterkühlungsdominierte Betriebsstrategien. Aufgrund sicherer Handhabung, überwiegend kongruenten Schmelzens und eines ausgeprägten, extern auslösbaren unterkühlten Zustands wurde SAT ausgewählt, während CCH wegen Hygroskopizität, Korrosivität, inkongruentem Schmelzen und geringerer Regelbarkeit ausgeschlossen wurde. Die experimentellen Untersuchungen konzentrierten sich auf Hydratstabilität, mechanische Robustheit und thermisches Verhalten von SAT. Der Wassergehalt wurde mittels Karl-Fischer-Titration und Halogen-Feuchteanalyse bestimmt, wobei eine deutliche methodenabhängige Abweichung festgestellt wurde; die Karl-Fischer-Methode wurde als Referenz festgelegt.

Die mechanische Stabilität von geschmolzenem SAT wurde mittels analytischer Zentrifugation (LumiSizer) untersucht und zeigte auch unter erhöhten Zentrifugalbelastungen keine Anzeichen makroskopischer Kristallisation. Thermische Zyklierungsexperimente mit einem EasyMax-Reaktor und Heat-Flow-Kalorimetrie zeigten, dass tiefe Abkühlung Unterkühlung auslöst, eine vollständige Kristallisation jedoch allein durch Temperaturführung innerhalb kurzer Zykluszeiten nicht zuverlässig erreicht wird. Dies unterstreicht die Notwendigkeit aktiver Auslösemechanismen und/oder verlängerter Tieftemperatur-Haltezeiten.

Insgesamt bestätigen die Ergebnisse die Eignung eines unterkühlungsbasierten experimentellen Ansatzes mit SAT und liefern zentrale Randbedingungen für das Payload-Design, darunter die Verifikation des Wassergehalts, die Robustheit gegenüber startrelevanten mechanischen Belastungen sowie die Integration kontrollierter Nukleationsmechanismen zur Sicherstellung der Kristallisation während der Mikrogravitationsphase.

Lucerne, 05. January 2026

© Enderli Julia, Lucerne School of Engineering and Architecture

Table of Content

1	Introduction	1
1.1	Background	1
1.2	Problem Description.....	2
1.3	Project Aim and Objectives.....	3
1.4	Report Structure Outlook	3
2	Literature Review	5
2.1	Phase Change Materials	5
2.1.1	Inorganic vs. Organic PCMs	6
2.1.1.1	Sodium Acetate Trihydrate – SAT	6
2.1.1.2	Calcium Chloride Hexahydrate – CCH.....	8
2.2	Crystallization	9
2.3	Supercooling.....	9
2.3.1	Triggers.....	10
2.4	Research Gap and Advancement of Field	11
3	Methodology	13
3.1	Research Strategy	13
3.2	Decision Process.....	13
3.2.1	Assessment criteria.....	14
3.2.2	Final Solution Selection	19
3.3	Laboratory Testing.....	20
3.3.1	Sample Preparation.....	20
3.3.2	Water Content Analysis	21
3.3.2.1	Metrohm 915 KF Ti-Touch Titrator	22
3.3.2.2	Halogen Moisture Analyzer.....	24
3.3.3	LumiSizer	26
3.3.4	EasyMax 102 with HFCal extension.....	27
3.4	Experimental Matrix.....	29

4	Results	32
4.1	Water Content Analysis – Experiment 1 and 2.....	32
4.2	LumiSizer - Experiment 3	34
4.3	EasyMax – Experiment 4 and 5	36
5	Discussion of Results	39
5.1	Experiment 1 and 2.....	39
5.2	Experiment 3	39
5.3	Experiment 4 and 5.....	41
6	Conclusion.....	43
7	Recommendations and Outlook	45
7.1	Implications of Laboratory Results for Microgravity Experiments	45
7.2	Future Experiment Setup on MASER Sounding Rocket	45
7.3	Design Constraints and Open Challenges	46
8	References	47
9	Appendix	51
A	Declaration of the Use of AI-based Tools	52
B	Table of Contents of Digital Appendix.....	53
B.1	Full Experimental Matrix.xls	53
B.2	Proposal_TripleF (Source_Worlitschek et al_nd).pdf.....	53
B.3	Experiment 1_Methrom 915_doku.pdf.....	53
B.4	Experiment 3_LumiSizer_full doku.pdf.....	53
B.5	Experiment 3_Sample 8_LumiSizer_doku sample 8.pdf.....	53
B.6	Experiment 4_EasyMax	53
B.7	Experiment 5_EasyMax	53
B.8	HalogenDryer_Experiments	53
B.9	EasyMax_Other Experiments.....	53
B.10	LumiSizer_Other Experiments.....	53
B.11	Other Experiments.....	53

Figures

Figure 1: Phase Change Diagram of SA and H ₂ O (Ma et al., 2017)	8
Figure 2: Liquid Sample Preparation	20
Figure 3: The Methrom 915 KF Ti-Touch Titrator.....	22
Figure 4: The Mettler Toledo HX204 Halogen Moisture Analyzer	24
Figure 5: The LumiSizer	26
Figure 6: The EasyMax	27
Figure 7: Sample before the moisture analysis.	33
Figure 8: Sample after the moisture analysis	33
Figure 9: Water Content Analysis over time	33
Figure 10: Instability Index over time	34
Figure 11: Radial Transmission Profiles	35
Figure 12: Temperature over Time Profile of Experiment 4	36
Figure 13: Temperature over time of Experiment 5	37

Tables

Table 1: Assessment criteria SAT vs CCH (Ma et al., 2017; Wang et al., 2019)	14
Table 2: Comparison SAT vs. CCH (Ma et al., 2017; Wang et al., 2019)	15
Table 3: Assessment criteria supercooling vs. cooling-power (Machida et al., 2017)	17
Table 4: Cooling Power vs. Supercooling (Machida et al., 2017).....	18
Table 5: Excerpt of the Experimental Matrix	31
Table 6: Results of Experiment 1 - Metrohm 915 KF Ti-Touch Titrator	32

Abbreviations and Acronyms

Abbreviation / Acronym	Definition
CCH	Calcium Chloride Hexahydrate
ESA	European Space Agency
FACT	Fully Automatic Calibration Technology
HFCal	Heat-Flow Calorimetry
LHTES	Latent Heat Thermal Energy Storage
NIR	Near-InfraRed
PCM(s)	Phase Change Material(s)
SA	Sodium Acetate
SAT	Sodium Acetate Trihydrate
TES	Thermal Energy Storage
T _j	Jacket Temperature
T _r	Sample Temperature

1 Introduction

This chapter introduces the context, motivation, and objectives of the present study. It outlines the relevance of phase change materials for thermal energy storage in space applications, identifies the key challenges associated with crystallization under terrestrial gravity, and highlights the need for experimental investigation under microgravity conditions. The chapter further defines the research problem, states the project aims, and provides an overview of the report structure.

1.1 Background

Future human exploration missions to the Moon and Mars place stringent demands on reliable and efficient thermal management systems. (Swedish Space Corporation, 2014) Spacecraft, planetary habitats, and surface vehicles are exposed to extreme and highly variable thermal environments, while mass, volume, and energy availability are strongly constrained. Phase change materials (PCMs) represent a promising solution for such applications, as they are capable of absorbing and releasing large amounts of thermal energy at nearly constant temperatures through reversible melting and solidification processes. (Ma et al., 2017; Swedish Space Corporation, 2014)

Inorganic salt hydrates, such as sodium acetate trihydrate (SAT) and calcium chloride hexahydrate (CCH), are of particular interest due to their high latent heat storage capacity, relatively low cost, non-flammability, and favorable melting temperatures for low- to medium-temperature thermal energy storage. (Wang et al., 2019) These materials have therefore been widely studied for terrestrial applications, including building energy systems and thermal buffering. However, their broader application is limited by long-term stability issues arising during repeated phase change cycles, including phase segregation, void formation, and incomplete crystallization. (Ma et al., 2017; Wang et al., 2019)

Under terrestrial gravity conditions, crystallization of salt hydrates is strongly influenced by buoyancy-driven convection, sedimentation, and density differences between phases. (Ma et al., 2017) These gravity-induced effects can lead to inhomogeneous crystal growth, separation of hydrate phases, and irreversible degradation of thermal performance. It is hypothesized that many of these limitations are not intrinsic material properties, but rather consequences of gravitational forces acting during solidification. In microgravity, where convection and sedimentation are largely suppressed, crystallization is expected to be governed predominantly by diffusion, potentially resulting in more homogeneous structures and improved reversibility. (Krämer, 2025; Ma et al., 2017)

Understanding the solidification behavior of PCMs under microgravity conditions is therefore of high relevance for both space and terrestrial applications. While previous microgravity studies have focused mainly on melting processes or on organic PCMs, experimental data on the solidification of complex inorganic salt hydrates in microgravity remain scarce. (Swedish Space Corporation, 2014) Addressing this knowledge gap is essential for the development of reliable thermal energy storage systems for long-duration space missions. (Krämer, 2025)

This Bachelor thesis is embedded in the context of an upcoming European Space Agency (ESA) sounding rocket experiment and contributes experimental groundwork required for its design and execution. (Worlitschek et al., n.d.) By investigating the crystallization behavior of SAT and CCH under controlled laboratory conditions, the project supports the preparation, parameter definition, and feasibility assessment of PCM solidification experiments in microgravity.

1.2 Problem Description

Despite their favorable thermophysical properties, salt hydrate PCMs suffer from several challenges that limit their reliability in practical applications. During solidification under Earth gravity, gravity-driven convection and sedimentation promote phase segregation, the formation of voids, and non-uniform crystal growth. (Ma et al., 2017) Over repeated melting–solidification cycles, these effects lead to a gradual loss of latent heat storage capacity and reduced reversibility of the phase change process. (Wang et al., 2019)

For space applications, these limitations pose a critical risk. Thermal management systems in spacecraft and planetary habitats must operate reliably over long durations without maintenance or material replacement. However, most existing experimental data on PCM behavior has been obtained under terrestrial gravity conditions, where gravitational effects obscure the fundamental mechanisms governing crystallization. (Swedish Space Corporation, 2014) As a result, it remains unclear to what extent segregation, supercooling, and void formation are inherent material properties or artefacts induced by gravity. (Krämer, 2025)

In addition, PCM crystallization is often associated with significant supercooling, particularly for salt hydrates such as SAT. Uncontrolled supercooling can delay solidification, reduce system predictability, and complicate experimental interpretation. For microgravity experiments, where available time and control authority are limited, precise definition of crystallization onset, completion criteria, and triggering mechanisms is essential. (Machida et al., 2017)

Before conducting experiments in a sounding rocket environment, it is therefore necessary to systematically characterize crystallization behavior under well-controlled laboratory conditions.

Key open questions include how fast crystallization proceeds, how supercooling can be reduced or controlled, how complete solidification can be defined experimentally, and which cooling and triggering methods are suitable within the constraints of rocket flight hardware.

Without this preparatory work, the design of a microgravity experiment would involve high uncertainty and increased risk of inconclusive or unusable results. The present project addresses this gap by generating experimental input required to design, parameterize, and de-risk PCM solidification experiments under space conditions. (Swedish Space Corporation, 2014)

1.3 Project Aim and Objectives

To investigate the crystallization behavior of selected phase change materials under controlled conditions and provide experimental input for the design of a sounding rocket payload.

- Determine crystallization onset, speed, and stability of sodium acetate trihydrate (SAT) and calcium chloride hexahydrate (CCH) under controlled laboratory conditions.
- Analyze the extent of supercooling and evaluate methods (e.g., seeding or mechanical triggers) to reduce it.
- Define criteria for when PCMs can be considered “fully solidified” for experimental purposes.
- Compare different probe sizes and cooling methods (e.g., Peltier elements) for suitability under rocket flight constraints.

The findings of this thesis are intended to support the design and parameter definition of a future microgravity experiment on a MASER sounding rocket.

1.4 Report Structure Outlook

This report is structured as follows. Chapter 2 introduces the theoretical background, focusing on phase change materials with particular emphasis on sodium acetate trihydrate and calcium chloride hexahydrate, as well as the concepts of crystallization and supercooling relevant to microgravity applications. Chapter 3 describes the methodological approach, including the decision process for material and operational strategy selection, laboratory testing methods, and the experimental matrix.

Chapter 4 presents the experimental results obtained from water content analysis, stability assessment using analytical centrifugation, and thermal cycling experiments.

Chapter 5 discusses these results in relation to the research objectives, interpreting the observed behavior of supercooling, crystallization stability, and mechanical robustness under space-relevant conditions. Chapter 6 concludes the report by summarizing the key findings and their implications for the feasibility of controlled crystallization experiments in microgravity.

Finally, Chapter 7 provides recommendations and an outlook for future work, outlining design considerations, experimental improvements, and remaining challenges for the implementation of phase change material experiments on a sounding rocket platform.

2 Literature Review

This chapter delves into the theoretical and experimental foundations of phase change materials, with a particular focus on inorganic salt hydrates relevant for thermal energy storage applications. It begins by outlining the fundamental principles of phase change behavior and latent heat storage, establishing a basis for understanding how these materials enable efficient thermal management.

Following this conceptual grounding, the chapter examines key material classes, comparing organic and inorganic phase change materials and highlighting the specific properties of sodium acetate trihydrate and calcium chloride hexahydrate. Particular attention is given to crystallization mechanisms and supercooling behavior, which critically influence material performance and controllability.

Next, the chapter reviews existing experimental studies on crystallization and solidification of salt hydrate PCMs under terrestrial conditions, identifying known challenges such as phase segregation, incongruent melting, and delayed nucleation. Where available, insights from reduced-gravity and microgravity research are discussed to illustrate how gravitational effects alter crystallization dynamics.

The final section identifies a persistent research gap in the experimental understanding of salt hydrate crystallization under microgravity conditions, particularly regarding controlled supercooling and nucleation. By addressing these aspects, this chapter establishes the scientific basis for the experimental approach and material selection developed in the subsequent chapters.

2.1 Phase Change Materials

PCMs are substances that can exist in at least two different phases and be repeatedly switched between them. This study focuses on PCMs that undergo transitions between the solid and the liquid phase. In the liquid phase, short-range order is preserved such that intermolecular distances are well defined, while molecular orientations and bond angles remain largely disordered. In contrast, the solid phase exhibits long-range order, with both intermolecular distances and bond angles arranged in a regular, lattice-like structure. These structural differences lead to distinct physical properties, including mass density, viscosity, thermal conductivity, and optical behavior. (Shamseddine et al., 2022)

PCMs are primarily used for energy storage, leveraging the repeatability of their phase transitions. They are stable for many years within their operating temperature ranges, which generally span $-5\text{ }^{\circ}\text{C}$ to $190\text{ }^{\circ}\text{C}$ depending on the material and application.

In practice, solid-liquid and liquid-solid transitions are the most used because they offer high latent heat storage and reversible cycling. Although liquid-gas transitions provide higher heats of transformation, they are impractical for thermal storage due to large volume or high-pressure requirements. Solid-solid transitions are limited by slow kinetics and low transformation enthalpies. At the phase change temperature, PCMs absorb or release latent heat while maintaining nearly constant temperature, making them suitable for thermal management. Applications include building materials, solar energy systems, waste heat recovery, refrigeration, textiles, heat pumps, battery and microelectronics thermal management, photovoltaic thermal systems, and greenhouse climate control. (Shamseddine et al., 2022)

2.1.1 Inorganic vs. Organic PCMs

PCMs are generally classified as organic or inorganic, each with unique properties, advantages, and limitations. (Shamseddine et al., 2022)

Organic PCMs, such as hydrocarbons (C_nH_{2n+2}), lipids, and sugar alcohols, exhibit minimal supercooling, congruent melting, self-nucleating behavior, chemical stability, and non-reactivity. They are resistant to phase segregation, ensuring reliable performance over repeated thermal cycles. Their limitations include low thermal conductivity in the solid state, relatively low volumetric latent heat storage, high purification costs that can reduce phase transition sharpness, and flammability, which requires specialized containment in some applications. (Shamseddine et al., 2022)

Inorganic PCMs, typically salt hydrates ($M_xN_y \cdot nH_2O$) or metallic systems, offer higher volumetric latent heat storage, sharp melting points, high thermal conductivity, high heat of fusion, non-flammability, low cost, and good availability. Notable examples include SAT and CCH, which are widely used for thermal energy storage. However, inorganic PCMs can suffer from incongruent melting, phase separation, corrosion, large volume changes upon phase transition, and supercooling, which often requires nucleating agents. These agents may lose effectiveness over repeated cycles, limiting long-term reliability. The choice between organic and inorganic PCMs involves balancing energy density, stability, cost, and safety according to the application. (Wang et al., 2019)

2.1.1.1 Sodium Acetate Trihydrate – SAT

Sodium acetate trihydrate ($CH_3COONa \cdot 3H_2O$) is an inorganic salt hydrate PCM widely used for medium-temperature latent heat storage applications such as reusable heat packs, domestic hot water systems, and solar thermal integration, owing to its melting point of approximately 58 °C and a latent heat of fusion of about 250–260 kJ/kg. (Ma et al., 2017; Sharma et al., 2009)

During phase transition, the density of SAT decreases from approximately 1.45 g/cm^3 in the solid phase to about 1.28 g/cm^3 in the liquid phase, corresponding to a moderate volume change of 8–10 %. (Ma et al., 2017; Sharma et al., 2009) Although SAT exhibits relatively low thermal conductivity ($0.2\text{--}0.3 \text{ W/m}\cdot\text{K}$), leading to slower heat transfer than materials such as calcium chloride hexahydrate, this limitation is compensated by its high stability and well-controlled crystallization behavior. (Ma et al., 2017; Sharma et al., 2009)

A key characteristic of SAT is its pronounced tendency to supercool, allowing the material to remain in a metastable liquid state typically 10–20 K below its melting point without spontaneous crystallization. (Machida et al., 2017) This behavior is governed by the absence of nucleation sites and is strongly influenced by purity, container surface properties, and cooling rate, with smooth and clean surfaces promoting deeper supercooling while impurities or surface irregularities may trigger premature crystallization. The ability to maintain a supercooled state over extended periods makes SAT particularly attractive for applications requiring delayed heat release, including space experiments where unwanted solidification during launch must be avoided. (Ma et al., 2017)

Once nucleation is initiated, crystallization propagates rapidly through the liquid in an exothermic, diffusion-limited process, with complete solidification typically occurring within a few minutes depending on sample geometry and thermal boundary conditions. Several reliable triggering mechanisms exist, including the introduction of seed crystals, mechanical impact, localized thermal pulses, ultrasonic excitation, or microcapsules containing nucleation agents, providing reproducible external control of crystallization that distinguishes SAT from many other PCMs (Ma et al., 2017).

SAT is commonly characterized using Differential Scanning Calorimetry to determine melting and crystallization temperatures and latent heat, complemented by T-history methods for larger sample volumes. Optical or infrared imaging enables visualization of the crystallization front, while repeated cycling tests assess the stability and reproducibility of the supercooled state. These techniques form the basis for optimizing experimental conditions under both terrestrial and microgravity environments. (Ma et al., 2017)

In microgravity, the absence of buoyancy-driven convection alters crystallization dynamics, resulting in diffusion-controlled nucleation and crystal growth with more uniform solidification fronts, although changes in nucleation probability and growth rates may also occur. These effects make SAT a valuable model system for studying fundamental nucleation kinetics under reduced-gravity conditions. (Ma et al., 2017)

For space applications, risks such as premature crystallization, incomplete solidification within limited experimental timeframes, and remelting during re-entry must be addressed through careful purification, optimized container design, and strict temperature control. When these measures are implemented, sodium acetate trihydrate emerges as an excellent PCM for controlled supercooling and nucleation studies in microgravity, combining reliable triggering, clear thermal signatures, manageable volume changes, and strong scientific relevance (Ma et al., 2017).

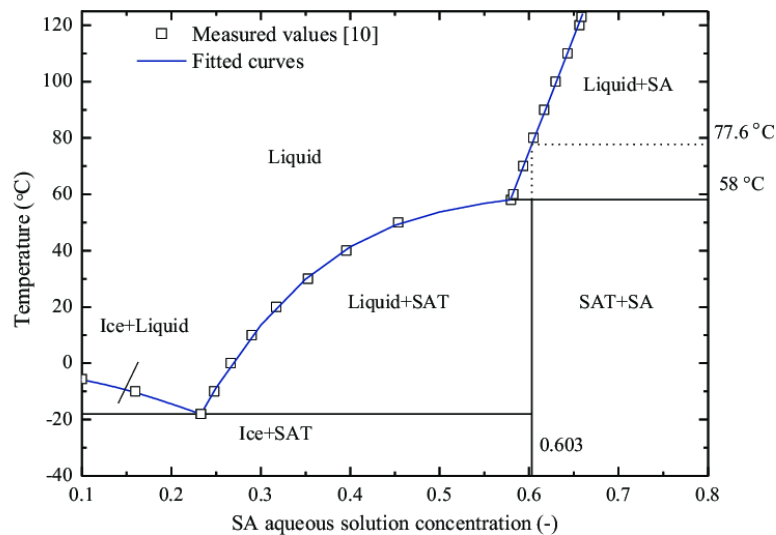


Figure 1: Phase Change Diagram of SA and H₂O (Ma et al., 2017)

2.1.1.2 Calcium Chloride Hexahydrate – CCH

Calcium chloride hexahydrate (CaCl₂·6H₂O) is a widely studied inorganic salt hydrate used for latent heat thermal energy storage due to its low cost, non-flammability, and favorable thermo-physical properties. It exhibits a melting temperature of approximately 28 °C and a latent heat of fusion of about 159–160 J/g, resulting in a high volumetric energy storage density well suited for low-temperature thermal storage applications such as building energy management and passive cooling systems (Wang et al., 2019).

Despite these advantages, pure CCH suffers from several intrinsic drawbacks that limit its reliability, particularly under conditions requiring precise crystallization control. The material exhibits pronounced supercooling, often exceeding 10–14 K, and undergoes incongruent melting, which leads to phase segregation, liquid leakage, and degradation of thermal performance over repeated cycles (Wang et al., 2019). In addition, CCH is hygroscopic and corrosive, imposing strict requirements on container materials and sealing integrity.

To mitigate these limitations, extensive research has focused on material modification strategies rather than external crystallization control.

The addition of nucleating agents, most commonly strontium chloride hexahydrate ($\text{SrCl}_2 \cdot 6\text{H}_2\text{O}$), has been shown to significantly reduce supercooling when applied at optimized concentrations (~ 3 wt%), while porous matrices and conductive additives are frequently used to suppress leakage and improve heat transfer (Wang et al., 2019). While these approaches improve terrestrial performance, they introduce additional material complexity and reduce experimental controllability.

From a microgravity perspective, these characteristics make CCH less suitable for controlled crystallization experiments. Its tendency toward spontaneous nucleation, reliance on internal material modification rather than external triggering, and sensitivity to composition and hydration state limit its applicability in short-duration experiments with constrained control authority. As a result, CCH is better suited for applications prioritizing rapid heat release and high cooling power under gravity-dominated conditions, rather than for supercooling-based, on-demand crystallization studies in microgravity environments (Wang et al., 2019).

2.2 Crystallization

Crystallization is the transition of a PCM from liquid to solid, releasing latent heat absorbed during melting. This process begins with nucleation, either spontaneous or triggered by impurities, surfaces, or additives. The rate and uniformity of crystallization affect thermal performance; uneven or slow crystallization may cause localized overheating or incomplete energy release. (Machida et al., 2017)

Controlling crystallization is crucial for PCMs prone to supercooling. Methods include seeding, adding nucleating agents, or encapsulation, all of which enhance crystallization reliability and improve TES efficiency. (Machida et al., 2017)

2.3 Supercooling

The delay in the start of solidification is called supercooling and takes place whenever a PCM undergoes a phase change from liquid to solid. That means the PCM remains liquid below its equilibrium solidification temperature. The degree of supercooling is the difference between melting and nucleation temperatures. During this metastable state, latent heat release is delayed until nucleation occurs, which can cause sudden temperature spikes. (Machida et al., 2017; Shamseddine et al., 2022)

In Thermal Energy Storage (TES), supercooling is usually undesirable because it delays heat delivery and reduces useful latent heat, whereas in biological or preservation applications it can prevent ice formation.

Factors affecting supercooling include cooling rate, container size and surface properties, impurities, thermal history, and thermal conductivity. Mitigation strategies include nucleating agents, modified cooling conditions, and microencapsulation, which can enhance heat transfer but may also increase supercooling. Supercooling is complex and application-dependent, potentially improving or impairing PCM performance. (Machida et al., 2017; Shamseddine et al., 2022)

2.3.1 Triggers

CCH

Calcium chloride hexahydrate generally requires assisted nucleation to ensure reliable and timely crystallization due to its tendency to supercool. In pure form, spontaneous nucleation is unpredictable and often delayed by more than 10 K below the equilibrium freezing temperature. The most established triggering approach is the addition of nucleating agents, particularly isomorphous salt hydrates such as strontium chloride hexahydrate ($\text{SrCl}_2 \cdot 6\text{H}_2\text{O}$), which provide crystallographic compatibility and reduce the energy barrier for nucleation. At optimized concentrations (≈ 3 wt%), these additives significantly suppress supercooling and promote uniform crystal growth. (Wang et al., 2019)

In composite PCMs, solid surfaces within porous matrices (e.g. expanded perlite, graphite-based additives) act as heterogeneous nucleation sites and further stabilize crystallization. Mechanical triggers are generally ineffective for CCH, and thermal triggering requires cooling well below the melting point, which limits precise timing. Consequently, crystallization control in CCH relies primarily on material modification rather than external, on-demand triggers, making it suitable for applications prioritizing rapid heat release over delayed activation. (Wang et al., 2019)

SAT

Sodium acetate trihydrate exhibits a pronounced and stable supercooled state, allowing crystallization to be triggered externally and on demand. Unlike CCH, SAT can remain liquid 10–20 K below its melting temperature for extended periods without spontaneous nucleation, provided impurities and surface defects are minimized. This strong metastability enables the use of active triggering mechanisms to precisely control the onset of crystallization. (Ma et al., 2017; Machida et al., 2017)

The most common trigger is the introduction of seed crystals, which immediately initiate crystallization and rapid latent heat release.

Mechanical triggers, such as impact or flexing of a metal disc, are also effective by locally disturbing the liquid structure and generating nucleation sites. Additional methods include localized thermal pulses, ultrasonic excitation, and microencapsulated nucleators that rupture under mechanical or thermal stress. These trigger mechanisms are highly reproducible and allow accurate control of crystallization timing, making SAT particularly suitable for applications requiring delayed heat release, including controlled laboratory experiments and microgravity environments. (Ma et al., 2017; Machida et al., 2017)

2.4 Research Gap and Advancement of Field

Research on inorganic salt hydrate phase change materials has predominantly focused on reducing supercooling and improving cycling stability for terrestrial thermal energy storage applications. Common strategies include the use of nucleating agents, composite structures, encapsulation, and enhanced heat transfer to promote rapid and reliable crystallization under gravity-dominated conditions. In this context, supercooling is generally treated as an undesirable effect that should be minimized. (Krämer, 2025; Swedish Space Corporation, 2014)

However, significantly less attention has been given to the intentional use of supercooling as an operational state, particularly under reduced-gravity conditions. In microgravity, buoyancy-driven convection, sedimentation, and density-driven phase separation are strongly suppressed, which fundamentally alters crystallization behavior. As a result, material limitations observed on Earth may not represent intrinsic properties but rather gravity-induced effects. (Krämer, 2025; Swedish Space Corporation, 2014)

Existing microgravity studies on phase change materials have mainly addressed melting processes or organic PCMs, while experimental investigations of solidification and crystallization of inorganic salt hydrates remain scarce. Moreover, there is limited experimental data on how supercooled salt hydrates behave under the combined thermal and mechanical boundary conditions relevant to sounding rocket missions, including launch acceleration, short microgravity durations, and constrained thermal control. (Swedish Space Corporation, 2014)

This lack of experimental groundwork complicates the design of space-based crystallization experiments. Open questions remain regarding the stability of the supercooled state prior to microgravity, the controllability and detectability of crystallization onset within short experimental windows, and the suitability of laboratory-scale indicators for predicting in-flight behavior. (Swedish Space Corporation, 2014)

The present thesis addresses this research gap by shifting the perspective from suppressing supercooling to characterizing it as a controllable state for microgravity experimentation.

Through a structured comparison of sodium acetate trihydrate and calcium chloride hexahydrate, an evaluation of supercooling-dominated versus cooling-power-driven operation, and targeted laboratory experiments on water content, mechanical stability, and thermal response, this work provides essential experimental input for the design and risk reduction of a future sounding rocket experiment.

3 Methodology

This chapter presents the methodological approach employed in this study to achieve the project's core objectives, including material selection, experimental design, and laboratory-based characterization of phase change materials. It outlines the overall research strategy and provides the rationale for the chosen experimental methods and decision criteria.

To address these objectives, a structured and predominantly quantitative approach was adopted, combining systematic literature analysis with targeted laboratory experiments. The methodology includes a decision process for selecting the phase change material and operational strategy, followed by experimental investigations of water content, mechanical stability, and thermal behavior using Karl Fischer titration, analytical centrifugation, and heat-flow calorimetry.

Each method was selected to generate data directly relevant to the design of a microgravity experiment and to reduce uncertainty in material behavior under space-relevant conditions. The experimental procedure and data evaluation are described in detail in the following subchapters. The methodological framework was continuously reviewed and refined through regular discussions with the project supervisors, and all experimental activities were conducted within the defined project timeline.

3.1 Research Strategy

The literature review followed a systematic approach to identify and analyze existing research related to PCMs with a special focus on SAT and CCH and their characteristics, applications, triggers and use cases. The objective was to gather insights into already existing knowledge, known challenges and outcomes relevant to use SAT and CCH in the proposed experiment.

The literature search was conducted across major academic databases, including Google Scholar and ScienceDirect. Search terms were developed based on the key concepts of the study, using Boolean operators and keyword combinations such as "PCM", "SAT", "CCH", "supercooling", "cooling power", and many more. Reference lists of key papers were also reviewed for additional sources.

3.2 Decision Process

In this subchapter the decision process from the beginning until the decision which PCM to choose as well as the choice to set the focus on cooling power or supercooling is shown.

3.2.1 Assessment criteria

Based on the requirements defined in Chapter 1.2 and Chapter 1.3, a set of assessment criteria was derived to enable a structured comparison between (i) the two phase change materials and (ii) the alternative operational strategies. The criteria focus on thermophysical performance, operational robustness, experimental feasibility, and system-level relevance for low-temperature LHTES.

SAT vs. CCH

Table 1: Assessment criteria SAT vs CCH (Ma et al., 2017; Wang et al., 2019)

No.	Requirement	Description	Weighting
1	Latent Heat Storage Capacity	Ability of the PCM to store thermal energy per unit mass and volume.	0.15
2	Phase change temperature suitability	Compatibility of the melting and solidification temperatures with low-temperature thermal storage applications.	0.10
3	Super cooling behavior and controllability	Extent of supercooling and the feasibility of reproducible nucleation control	0.20
4	Phase stability and congruent melting	Tendency towards phase segregation, dehydration, or long-term degradation during repeated cycling	0.20
5	Operational robustness and handling	Sensitivity to impurities, water content variations and container interaction.	0.15
6	Experimental and system integration feasibility	Suitability for controlled laboratory experiments and relevance for system-level demonstrations	0.20

As an additional decision tool, the following comparison table was created where the most important parameters of SAT and CCH are listed (Ma et al., 2017):

Table 2: Comparison SAT vs. CCH (Ma et al., 2017; Wang et al., 2019)

Parameter	Sodium Acetate Trihydrate (SAT)	Calcium Chloride Hexahydrate (CCH)
Formula	$\text{CH}_3\text{COONa} \cdot 3\text{H}_2\text{O}$	$\text{CaCl}_2 \cdot 6\text{H}_2\text{O}$
Melting Point	~ 58 °C	~ 29-30 °C
Latent Heat	~ 250 - 260 kJ/kg	~ 190 kJ/kg
Density (solid/liquid)	1.45 / 1.28 g/cm ³	1.71 / 1.56 g/cm ³
Thermal Conductivity	0.2 - 0.3 W/m · K	0.54 W/m · K
Tendency to Supercool	High (up to > 20K)	Low (≈ 3-5K)
Phase Stability	High if pure and sealed	Prone to incongruent melting
Cycle Stability	Very good	Degrades after few cycles
Safety / Handling	Benign	Hygroscopic and corrosive

The following statements were developed from Table 1 and Table 2:

- Due to the larger temperature margin between laboratory ambient conditions ($\approx 23\text{--}24$ °C) and its melting point, SAT remains clearly in the solid phase and is therefore easier to thermally control than CCH whose melting temperature lies close to ambient conditions.
- SAT exhibits predominantly congruent melting behavior, preserving compositional homogeneity, whereas CCH undergoes incongruent melting, leading to phase segregation and a progressive loss of effective latent heat storage capacity.
- Due to its low supercooling stability, CCH is prone to spontaneous nucleation and would likely crystallize prematurely during launch or ascent if transported in the liquid state, preventing controlled crystallization during the microgravity phase.
- SAT is safer to handle in small-scale laboratory setups and rocket payloads whereas CCH's high hygroscopicity and corrosive nature pose increased risks to containment integrity and payload components.
- Although CCH offers higher thermal conductivity and faster crystallization, SAT provides more reproducible crystallization allowing clear observation fronts in microgravity.

Supercooling vs. Cooling Power

Table 3: Assessment criteria supercooling vs. cooling-power (Machida et al., 2017)

No.	Requirement	Description	Weighting
1	Energy Storage Density	Ability to maximize stored latent heat per cycle	0.20
2	Discharge controllability and response time	Predictability and speed of heat release upon activation	0.20
3	System complexity	Required control mechanisms, triggering methods, and auxiliary components	0.15
4	Reliability and Reproducibility	Sensitivity to disturbances, vibration, and environmental conditions	0.15
5	System simplicity	Suitability for stationary systems versus experimental, mobile, or microgravity environments	0.10
6	Scientific insight potential	Ability to generate fundamental insights into crystallization and phase-change mechanisms under microgravity through controlled and observable system behavior.	0.20

Analogous to the supplementary comparison for SAT and CCH (Table 2), the following Table 4 presents a structured comparison of key parameters associated with cooling power and supercooling (Machida et al., 2017):

Table 4: Cooling Power vs. Supercooling (Machida et al., 2017)

Aspect	Cooling Power	Supercooling
Goal	Control phase transition by temperature gradient	Control phase transition by nucleation control
Mechanism	Force crystallization by rapid cooling below melting temperature	Maintain metastable liquid state below melting temperature until triggered
Advantage	Precise thermal timing	Long storage of liquid without crystallization
Risk	Premature freezing if overshoot	Failure to or premature crystallize or delayed nucleation
Trigger Type	Thermal (cooling power)	Mechanical / seeding / ultrasonic
System Demand	High cooling rate & power	High purity & vibration stability

The following statements were developed from Table 3 and Table 4:

- Supercooling-based operation allows thermal energy to be stored prior to launch and released exclusively during the microgravity phase, enabling temporal decoupling of charging and discharging which is not achievable with cooling-power-driven operation.
- Cooling-power-driven strategies rely on continuous heat extraction and steady thermal gradients, both of which are strongly altered under microgravity due to the absence of buoyancy-driven convection.
- Supercooling enables higher effective energy storage density within the limited sample volume of sounding-rocket payloads whereas cooling-power-driven operation continuously dissipates heat and underutilizes the short microgravity window.
- Although cooling-power-driven systems are generally more robust against mechanical disturbances, their continuous discharge limits controllability and reduces experimental flexibility under flight conditions.

- Supercooling-based operation enables controlled nucleation and clear observation of crystallization dynamics, providing higher scientific insight into phase-change behavior under microgravity.

3.2.2 Final Solution Selection

SAT or CCH

Due to the larger temperature margin between laboratory ambient conditions ($\approx 23\text{--}24\text{ }^\circ\text{C}$) and its melting point, SAT remains clearly in the solid phase and is therefore easier to thermally control than CCH whose melting temperature lies close to ambient conditions. SAT exhibits predominantly congruent melting behavior, maintaining compositional homogeneity whereas CCH tends to melt incongruently, leading to phase segregation and a reduction in effective latent heat storage capacity. Owing to its low supercooling stability, CCH is prone to spontaneous nucleation and would likely crystallize prematurely during launch or ascent if transported in the liquid state, preventing controlled crystallization during the microgravity phase. Furthermore, SAT is safer to handle in small-scale laboratory environments and rocket payloads, while CCH's hygroscopic and corrosive properties increase risks to containment and payload components. Although CCH offers higher thermal conductivity and faster crystallization kinetics, SAT provides significantly more reproducible crystallization behavior, enabling clear observation of solid-liquid interface dynamics under microgravity conditions. (Ma et al., 2017; Wang et al., 2019; Machida et al., 2017)

Supercooling or Cooling Power

Based on microgravity-specific assessment, a supercooling-dominated operational strategy is selected for the MASER experiments. This approach maximizes latent heat utilization within the constrained payload volume, allows intentional triggering during the microgravity phase, and enables direct observation of crystallization phenomena that cannot be isolated under terrestrial conditions. While cooling-power-driven operation offers greater robustness in stationary systems, its continuous heat release and reduced scientific observability make it less suitable for short-duration microgravity experimentation. (Ma et al., 2017; Wang et al., 2019; Machida et al., 2017)

Based on this assessment, calcium chloride hexahydrate was excluded from the experimental campaign. Although CCH was evaluated during the literature review and decision process, no laboratory experiments were conducted with this material.

This decision was taken deliberately to reduce experimental risk and to focus experimental resources on sodium acetate trihydrate, which offers higher controllability, safer handling characteristics, and greater relevance for supercooling-based microgravity experiments.

Furthermore, the experimental investigation was explicitly limited to a supercooling-dominated operational strategy. Cooling-power-driven operation was assessed conceptually but was not investigated experimentally, as it relies on continuous heat extraction and steady thermal gradients that are strongly altered under microgravity conditions and offer limited scientific insight within the short duration of sounding-rocket experiments. Consequently, no further experimental investigation into cooling-power-based operation was pursued within the scope of this thesis.

3.3 Laboratory Testing

The selected laboratory methods directly address the functional and operational requirements derived from the microgravity experiment constraints described in Chapter 1.2 and the project objectives defined in Chapter 1.3. Each method was chosen to quantify a specific risk or uncertainty relevant to sounding-rocket operation, including hydration stability, mechanical robustness, and controllability of supercooling and crystallization.

3.3.1 Sample Preparation

For all experiments, sodium acetate trihydrate (SAT) samples were prepared using a standardized mass and preparation procedure to ensure comparability across methods. For solid-state investigations, crystalline SAT was weighed using the same analytical balance for all samples, with a target mass of $8.08 \text{ g} \pm 0.01 \text{ g}$. This approach ensured consistent sample volume and thermal mass while minimizing variability arising from mass-dependent effects. The solid samples were handled under laboratory ambient conditions and transferred directly to the respective analytical instruments.

For experiments requiring molten SAT, the same target mass ($8.08 \text{ g} \pm 0.01 \text{ g}$) was weighed on the same balance prior to melting to maintain consistency with the solid-state samples. The weighed material was then melted in a thermostated water bath at $80 \text{ }^\circ\text{C}$. A metal grid (see Figure 2) was placed inside the water bath to elevate the sample vessel,

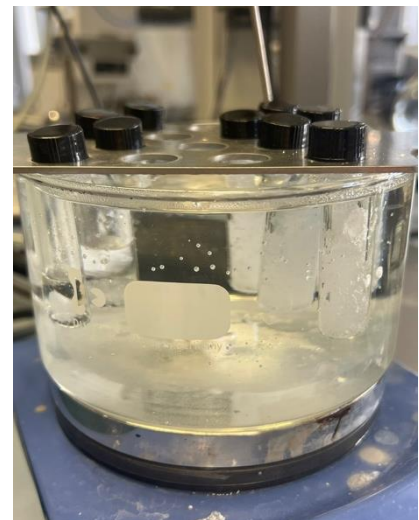


Figure 2: Liquid Sample Preparation

allowing the placement of a magnetic stirring bar at the bottom and ensuring uniform water temperature distribution around the container. During melting, the samples were continuously stirred at 400 rpm until complete liquefaction and visual homogeneity were achieved. This procedure ensured reproducible molten initial conditions and minimized temperature gradients and incomplete melting prior to subsequent experimental steps.

3.3.2 Water Content Analysis

For the water content analysis, two methods were applied. Here first, a summary of both techniques is provided, including their respective advantages and disadvantages, followed by a detailed description of the methodologies. (METTLER TOLEDO, n.d.-a; METTLER TOLEDO, n.d.-b)

Both the Metrohm 915 KF Titrator and the Mettler Toledo HX204 Halogen Moisture Analyzer are used for determining water content in samples, yet they differ fundamentally in principle, precision, and application scope. (Sharma et al., 2009; Skoog et al., 2014) The Metrohm 915 KF applies the Karl Fischer titration method, which chemically quantifies water through an iodine-sulfur dioxide reaction and offers high selectivity and accuracy, even at trace levels (<0.01%). (METTLER TOLEDO, n.d.-a; Skoog et al., 2014; Metrohm, n.d.) This makes it particularly suitable for materials where water is chemically or physically bound such as salt hydrates and PCMs. (METTLER TOLEDO, n.d.-a; Sharma et al., 2009) However, the method is more time-consuming, requires specialized reagents and maintenance, and is less practical for rapid routine screening.

In contrast, the Mettler Toledo HX204 operates on a thermogravimetric principle, measuring mass loss upon controlled heating with a halogen source. (METTLER TOLEDO, n.d.-b; Halogen Moisture Analyzer, n.d.) It allows fast, simple, and non-chemical determination of total moisture, ideal for process control or sample pre-testing, but lacks the precision to differentiate between bound and free water and may overestimate moisture in samples containing volatile compounds. (METTLER TOLEDO, n.d.-b; Skoog et al., 2014) In summary, the KF titrator excels in analytical accuracy and trace water detection while the HX204 analyzer offers operational speed and ease of use, making the two instruments complementary rather than directly substitutable in PCM characterization. (METTLER TOLEDO, n.d.-a; METTLER TOLEDO, n.d.-b; METTLER TOLEDO, 2025)

3.3.2.1 Metrohm 915 KF Ti-Touch Titrator



Figure 3: The Methrom 915 KF Ti-Touch Titrator

The quantification of the absolute water content in the PCM samples was performed via volumetric Karl Fischer titration using a Metrohm 915 KF Ti-Touch titrator. (METTLER TOLEDO, n.d.-a) This analytical method provides a precise and selective determination of both free and bound water, making it particularly suitable for salt hydrates such as SAT and CCH, where hydration state critically affects phase-change behavior. (Sharma et al., 2009)

Instrument Configuration

The 915 KF Ti-Touch is a fully integrated titration system that combines the burette, control unit, magnetic stirrer, and titration cell into a single compact device.

The instrument was operated with a 10 mL Dosino dosing unit, a double platinum electrode for electrochemical endpoint detection, and a Pt1000 temperature sensor for temperature monitoring. An integrated membrane pump enabled automated filling and emptying of the titration cell with anhydrous solvent, minimizing manual reagent handling and potential contamination. The instrument was connected to the local laboratory network via Ethernet, allowing for data storage, report generation, and traceable FDA-compliant PDF documentation without the need for an external computer.

Analytical Principle

The volumetric Karl Fischer method is based on the quantitative reaction of water with iodine and sulfur dioxide in an alcohol medium, catalyzed by a base. (Metrohm, n.d.; METTLER TOLEDO, n.d.-a; Skoog et al., 2014) The 915 KF Ti-Touch determines the endpoint potentiometrically by monitoring the current or voltage between the two indicator electrodes, operating in either voltametric (Ipol) or amperometric (Upol) mode. The endpoint corresponds to the stoichiometric consumption of iodine equivalent to the total water content of the sample. (METTLER TOLEDO, n.d.-a)

Measurement Procedure

Prior to each measurement series, the titration system was conditioned with the Karl Fischer reagent until the residual drift stabilized below $10 \mu\text{g H}_2\text{O}\cdot\text{min}^{-1}$, indicating a dry and equilibrated system. (Metrohm, n.d.)

Subsequently, approximately 0.1-1.0 g of homogenized PCM sample was introduced into the sealed titration vessel containing anhydrous methanol as solvent. The titration process commenced automatically upon sample addition and continued until the equivalence point was reached.

The water content (mass fraction) was automatically calculated by the Ti-Touch software according to the consumed titrant volume, reagent titer, and sample mass. Each measurement was carried out in triplicate to ensure statistical reliability, and all results were digitally stored and exported in PDF format to both a USB drive and the laboratory's data management system (LIMS).

Calibration and Quality Assurance

Instrument calibration and qualification followed the Metrohm IQ/OQ (Installation and Operational Qualification) procedures to guarantee traceable performance verification in accordance with regulatory standards. (Metrohm, n.d.) System suitability was routinely confirmed through titration of certified water standards, ensuring the accuracy and reproducibility of the volumetric measurements. Automatic electrode diagnostics and periodic maintenance further safeguarded the consistency of analytical results throughout the experimental campaign.

3.3.2.2 Halogen Moisture Analyzer

Purpose and Context

The Mettler Toledo HX204 halogen moisture analyzer was employed to quantify the total moisture content of the PCM samples. (METTLER TOLEDO, n.d.-d) This thermogravimetric method provides a rapid and robust measurement of free and loosely bound water, complementing the Karl Fischer titration used for chemically bound water determination. Accurate moisture quantification is essential for materials such as SAT and CCH where even slight deviations in hydration ratio can significantly alter melting behavior, latent heat storage, and supercooling tendencies. (Sharma et al., 2009) The HX204 was selected for its high precision, integrated quality management features, and suitability for laboratory research and process control applications. (METTLER TOLEDO, n.d.-d)



Figure 4: The Mettler Toledo HX204 Halogen Moisture Analyzer

Instrument Description

The HX204 is a high-performance halogen moisture analyzer designed for precise thermogravimetric determination of moisture content across a wide range of sample types. The system combines a high-resolution MFR weighing cell (readability: 0.1 mg / 0.001 % MC) with a fast-response halogen heating module operating between 40 °C and 230 °C in 1 °C increments. (METTLER TOLEDO, 2025) Its separated balance and heating unit architecture minimizes thermal interference, enabling optimal accuracy even at low moisture contents.

The analyzer integrates multiple drying profiles (standard, rapid, gentle, and stepwise drying) and supports method storage (up to 300 methods) and data logging (up to 3000 results). Real-time moisture curves, control charts, and the QuickPredict™ function allow prediction of final results in a fraction of the total measurement time, reducing analysis duration and supporting efficient decision-making.

Instrument performance and compliance are maintained through FACT (Fully Automatic Calibration Technology), SmartCal™ performance verification, and on-site testing of both heating and weighing units. (METTLER TOLEDO, 2025) An internal calibration routine ensures temperature and balance accuracy over time and temperature fluctuations.

The system further supports Ethernet, USB, and RS232 interfaces, user- and ID-management with access control, and direct report generation to A4 network printers or file servers. Its stainless-steel drying chamber, quartz-glass halogen lamp, and removable reflector assembly ensure thermal stability, durability, and easy cleaning.

Measurement Procedure

Before measurement, the instrument was allowed to equilibrate for at least 60 minutes under laboratory conditions (20-25 °C, RH < 60 %). The sample chamber was leveled and cleaned according to manufacturer instructions to prevent residue interference.

Approximately 1-2 g of homogenized PCM was distributed evenly on an aluminum sample pan to ensure consistent heat transfer. The drying temperature was selected based on pretests to achieve complete moisture removal without decomposing the hydrate, typically between 105 °C and 120 °C. (METTLER TOLEDO, n.d.-b) The analyzer automatically recorded the continuous (METTLER TOLEDO, n.d.-b; Halogen Moisture Analyzer, n.d.) change until the weight variation per time unit met the defined stability criterion (< 1 mg/30 s). The moisture content (%MC) was automatically calculated and displayed, along with the drying curve and predicted endpoint (QuickPredict™).

Each sample was measured in triplicate to verify repeatability (0.05 % at 2 g sample mass, 0.01 % at 10 g). Routine SmartCal™ tests were performed prior to the measurement series to confirm proper instrument function and heating uniformity. Following each run, the stainless-steel surfaces and halogen reflector were carefully cleaned using ethanol and lint-free wipes once the heating module had fully cooled.

Advantages for PCM Characterization

The HX204 moisture analyzer provides a rapid, non-destructive, and repeatable determination of total moisture, yielding complementary data to Karl Fischer titration. Its precise halogen drying system allows sensitive detection of water loss in salt hydrates without altering the crystalline structure during testing. The ability to predict results in real time and automatically document measurement data ensures high analytical efficiency and traceability. Combined with FACT and SmartCal verification, the system delivers reliable data for assessing PCM hydration state, stability, and long-term storage effects.

3.3.3 LumiSizer

Instrument Description

The LumiSizer Analytical Centrifuge is an advanced dispersion and stability analyzer designed to characterize the separation and sedimentation behavior of multiphase systems under accelerated conditions. (Van Baren, 2017) Manufactured by LUM GmbH (Berlin, Germany), the instrument combines centrifugal force and optical detection to determine particle migration, phase separation kinetics, and overall dispersion stability in real time. (LUM GmbH, n.d.)



Figure 5: The LumiSizer

The system operates by subjecting samples to controlled centrifugal fields of up to $2300 \times g$ while continuously measuring transmitted light through each sample cell using a multi-sample near-infrared (NIR) optical scanning system. The transmitted light intensity is recorded as a function of time and radial position, allowing for quantitative analysis of sedimentation, creaming, or clarification phenomena. (Van Brakel & Modry, 2017) Up to twelve samples can be analyzed simultaneously under identical conditions, providing reproducible and statistically robust data.

Temperature control within the measuring chamber enables isothermal or temperature-dependent experiments, making the device suitable for stability investigations of PCMs, emulsions, suspensions, and other multiphase formulations. The system software (SEPView®) provides advanced data processing tools for calculating sedimentation velocities, transmission profiles, and integral stability indices.

Measurement Procedure

Prior to measurement, liquid PCM samples were carefully filled into optically transparent polycarbonate cells to avoid air inclusions and ensure uniform optical path length. Each cell was sealed and mounted symmetrically within the rotor to prevent imbalance during rotation. The experimental parameters, centrifugal speed, acceleration time, duration, and temperature were predefined according to the specific viscosity and density of the investigated materials.

During the centrifugation process, transmission profiles were continuously recorded along the sample cell length. The obtained raw data were analyzed using the SEPView® software which converts spatially resolved transmission changes into temporal sedimentation or separation curves. These results enable quantification of phase separation rates, identification of multiple phases, and comparison of the relative stability of different formulations or preparation methods.

Advantages for PCM Characterization

The LumiSizer provides a unique advantage in accelerating long-term stability tests for salt-hydrate PCMs such as SAT and CCH. By applying centrifugal acceleration, processes that would normally take weeks under gravity can be reproduced within minutes, enabling a rapid assessment of material stability, phase segregation, or incongruent melting tendencies. (Van Baren, 2017)

Furthermore, the non-invasive optical detection allows monitoring of dynamic separation behavior without altering the sample composition, while the temperature control feature permits evaluation of thermally induced instabilities. Compared to conventional visual or gravimetric stability tests, the LumiSizer yields quantitative, reproducible, and high-resolution data, offering deeper insights into the material's internal structural stability and suitability for repeated melting-solidification cycles.

3.3.4 EasyMax 102 with HFCal extension

Instrument Description

The EasyMax and OptiMax HFCal systems are automated reaction calorimeters designed to quantify thermal effects during chemical reactions via Heat-Flow Calorimetry (HFCal). The instruments integrate a fully controlled reactor platform (EasyMax 102 / 102 LT / 402, OptiMax) with embedded heat-flow sensors that continuously measure the heat exchanged between the reaction mass and the thermostated reactor environment. (Van Baren, 2017) The



Figure 6: The EasyMax

calorimetric setup allows for precise determination of reaction enthalpies, heat release rates, and thermal stability parameters under isothermal or non-isothermal conditions. The systems include automated stirring, dosing interfaces, interchangeable reactor vessels, and integrated temperature control modules enabling accurate thermal and process-safety characterization across a range of chemical systems.

Measurement Principle

Heat-Flow Calorimetry is based on quantifying the heat flux between the reactor content and the thermostated jacket. The HFCal sensor measures the temperature difference between the process mass and the surrounding thermostat and converts this into a heat-flow signal via a calibrated heat-transfer coefficient (U-value).

Continuous acquisition of heat-flow data provides the instantaneous heat release or uptake (dQ/dt), while integrated heat curves allow determination of overall reaction enthalpies. Combined with controlled process parameters, temperature, stirring rate, dosing profiles, and reagent addition, the calorimeter enables reproducible monitoring of exothermic and endothermic events throughout the entire reaction trajectory.

Configuration and Operating Modes

The system supports a broad range of experimental configurations, including:

Isothermal calorimetry in which the reactor temperature is precisely maintained while heat-flow signals reveal reaction kinetics and thermal behavior.

Non-isothermal operation, enabling ramp or step temperature programs to investigate temperature-dependent reaction properties.

Semi-batch mode, where automated or manual dosing units introduce reactants while capturing transient heat spikes and cumulative enthalpies.

Batch mode, suitable for one-pot reactions with continuous thermal profiling.

Depending on the reactor model (EasyMax 102 / 102 LT / 402, OptiMax), the platform allows for variable working volumes, vessel materials, and cryogenic or elevated temperature operation. The systems also interface with Mettler Toledo automation modules for reagent addition and real-time data evaluation.

Experimental Procedure

A typical HFCal experiment proceeds as follows:

Reactor Setup: The reaction vessel is installed in the EasyMax or OptiMax base station, equipped with the HFCal heat-flow sensor. The vessel is charged with initial reagents and fitted with the appropriate stirring impeller and sensors (temperature, optionally pH or pressure).

Temperature Conditioning: The thermostat stabilizes the reactor at the target temperature. Baseline heat-flow is recorded to establish a reference signal.

Reaction Initiation: The process is started either by reagent addition (semi-batch) or by applying a programmed temperature profile (batch). The calorimeter continuously captures heat-flow signals throughout the reaction.

Data Acquisition: The system records heat release rate, cumulative heat, U-value normalization, and key reaction parameters. Automated algorithms correct for external disturbances and maintain thermal equilibrium.

Post-Processing: The collected HFCal data are analyzed to calculate reaction enthalpy, conversion-dependent heat release, thermal accumulation, and safety-relevant indices such as maximum temperature of the synthesis reaction (MTSR).

Advantages for PCM Characterization

For PCMs, HFCal calorimetry offers several specific analytical advantages:

Quantitative determination of phase-change enthalpy under realistic heating and cooling conditions enabling precise characterization of latent heat storage materials. (Sharma et al., 2009)

High-resolution detection of thermal transitions, including subcooling behavior, onset temperatures, and crystallization kinetics, critical for evaluating PCM stability. (Beaupère et al., 2020)

Assessment of reaction-induced thermal risks during PCM synthesis or hydration reactions, relevant for salt-hydrate systems such as SAT and CCH.

Reproducible thermal profiling under controlled isothermal or dynamic conditions, providing insight into heat-release asymmetry between melting and crystallization cycles.

Integration with automated dosing, supporting studies on nucleation triggers, additives, or water-content adjustments.

3.4 Experimental Matrix

Based on the laboratory methods described above and applied within this project, an experimental matrix was developed to systematically structure and evaluate the conducted experiments. (Montgomery, 2017) The matrix serves as a central overview of the experimental campaign, linking each experiment to its corresponding method, independent and controlled variables, measured outputs, and decision relevance for the design of a microgravity experiment.

Due to the large number of individual measurements and repetitions performed within this study, only a subset of representative experiments is presented in the experimental matrix included in this chapter. Specifically, one representative experiment per applied method was selected to illustrate the experimental approach and to facilitate interpretation of the results discussed in Chapters 4 and 5. These representative experiments capture the essential characteristics and outcomes of the respective methods and are therefore sufficient to support the methodological and analytical conclusions of this thesis.

Table 5 presents an excerpt of this experimental matrix, listing only those experiments that are directly relevant and further explained in the documentation. The experimental matrix, including all conducted experiments, the repetitions, and parameter variations can be seen in the digital Appendix 9B.1 for completeness and transparency.

By combining a concise overview in the main body of the report with a complete matrix in the appendix, this structure ensures clarity, traceability, and reproducibility of the experimental work while maintaining readability of the core document.

Table 5: Excerpt of the Experimental Matrix

EXP. ID	METHOD / INSTRUMENT	INDEPENDENT VARIABLES (IV)	CONTROLLED VARIABLES	PROGRAM / METHOD PARAMETERS	MEASURED OUTPUTS	EVALUATION CRITERIA	OUTCOME / DECISION RELEVANCE	DOCUMENTATION
E1	Karl Fischer Titration (Metrohm 915 KF Ti-Touch)	Measurement method (KF)	Reagent, solvent, endpoint detection, lab conditions	Volumetric KF; drift <10 µg/min; triplicate runs	Water content (% w/w)	Repeatability between runs; deviation from 39.7%	Reference method for hydration control	Ch. 4.1, Tab. 5
E2	Halogen Moisture Analyzer (Mettler Toledo HX204)	Measurement method (halogen drying)	Pan type, sample mass, ambient conditions	Drying at ~105–120 °C; endpoint <1 mg/30 s	Moisture curve (%MC vs time), final value	Agreement / deviation vs KF	Method suitability assessment	Ch. 4.1, Fig. 6–8
E3	Analytical Centrifugation (LumiSizer)	Centrifugal acceleration	Temperature, cell type, fill level	Stepwise: 1000 → 2000 → 4000 rpm	Instability index vs time	Absence of abrupt spikes → no phase separation	Launch/ascent robustness	Ch. 4.2, Fig. 9
E3-S8	LumiSizer – radial transmission (Sample 8)	Radial position	Same as E3	Same centrifuge program	Transmission vs radius	No propagating features → no bulk crystallization	Interpretation of optical artifacts vs real effects	Ch. 4.2, Fig. 10
E4	Thermal Cycling (EasyMax 102 + HFCal)	Tmin/Tmax range	Stirring, sensor position	3 trapezoidal cycles, ~10–95 °C	Tj, Tr vs time	No supercooling signatures	Baseline comparison	Ch. 4.3, Fig. 11
E5	Thermal Cycling + Supercooling Test (EasyMax 102 + HFCal)	Tmin extended to –20 °C	Same as E4	Multiple cycles, –20–95 °C	Temperature spikes, Tr response	Spikes = supercooling onset; no sustained plateau = no full crystallization	Need for active trigger	Ch. 4.3, Fig. 12

4 Results

This chapter presents the experimental results obtained from the laboratory investigations conducted in this study. The results are organized according to the applied experimental methods and focus on water content determination, mechanical stability assessment, and thermal response of sodium acetate trihydrate under controlled conditions. As already mentioned in Chapter 3.4 the presented experiments represent selected key cases. The results form the basis for evaluating supercooling behavior, crystallization stability, and experimental feasibility for microgravity applications and are discussed in detail in the subsequent chapter.

4.1 Water Content Analysis – Experiment 1 and 2

Following the melting attempt, the water content of the samples was determined using the two methods described in Chapter 3.3.2. (Metrohm, n.d.; METTLER TOLEDO, n.d.-b) The following section presents two representative experiments and their corresponding results.

Metrohm 915 KF Ti-Touch Titrator

The water content of the SAT samples was on one hand determined using a Karl Fischer titrator (Metrohm 915 KF Ti-Touch). For each measurement, approximately 0.45 g of the SAT solid crystals was weighed and analyzed according to the manufacturer's standard operating procedure for volumetric Karl Fischer titration. (Metrohm, n.d.) The titration was repeated at least three times. The following Table 6 shows the repetitions; the last value represents the mean of the repeated measurements of the first experiment.

Table 6: Results of Experiment 1 - Metrohm 915 KF Ti-Touch Titrator

No.	Weight	Result
1	0.4828 g	36.01%
2	0.4208 g	36.52%
3	0.4656 g	36.01 %
4	0.3525 g	37.35%
Mean Value	0.4304 g	<u>36.47%</u>

Halogen Moisture Analyzer

In Experiment 2, the water content of the SAT samples was determined using a halogen moisture analyzer. Approximately 1.02 g of solid SAT crystals were weighed and placed in a disposable aluminum sample pan, as shown in Figure 7. The prepared sample was then inserted into the moisture analyzer, and the measurement was initiated according to the standard operating procedure of the instrument. Figure 7 illustrates the SAT crystals after completion of the moisture analysis, showing the sample residue remaining in the aluminum pan.



Figure 7: Sample before the moisture analysis. Figure 8: Sample after the moisture analysis

The water content analysis in Figure 9 shows a continuous increase in measured moisture content over time, reaching a plateau after approximately 20 to 25 minutes. (Skoog et al., 2014) At the beginning of the measurement, only a small fraction of moisture is detected, followed by a steeper increase as the sample is progressively heated and water is released from the SAT crystals. As the measurement proceeds, the slope of the curve gradually decreases, indicating that most of the removable water has already been evaporated. (METTLER TOLEDO, n.d.-b) The stabilization of the curve toward the end of the measurement suggests that the drying process is complete and that the final moisture content of the sample, of 39.63% after 25:25min has been reached. (METTLER TOLEDO, n.d.-b)

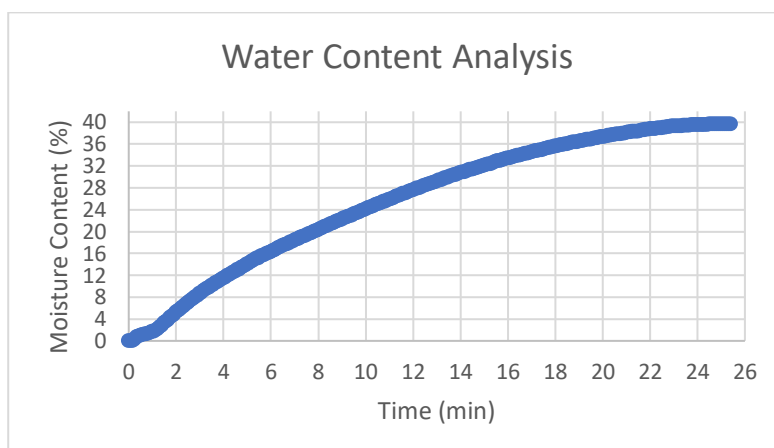


Figure 9: Water Content Analysis over time

Outcome

Although all samples used in both experiments originated from the same canister, notable differences in the measured water content were observed between the two analytical methods. (Skoog et al., 2014) The Karl Fischer Ti-Touch titrator indicated a deviation from the standard moisture content of approximately 3.23%, whereas the halogen moisture analyzer showed only a minor deviation of 0.03%. (Sharma et al., 2009) To verify the reproducibility of the measurements, both analyses were repeated, yielding very similar water content values. A deviation of approximately 3.23% was observed between the Karl Fischer titrator and the halogen moisture analyzer, while repeated measurements within each method showed high reproducibility.

4.2 LumiSizer - Experiment 3

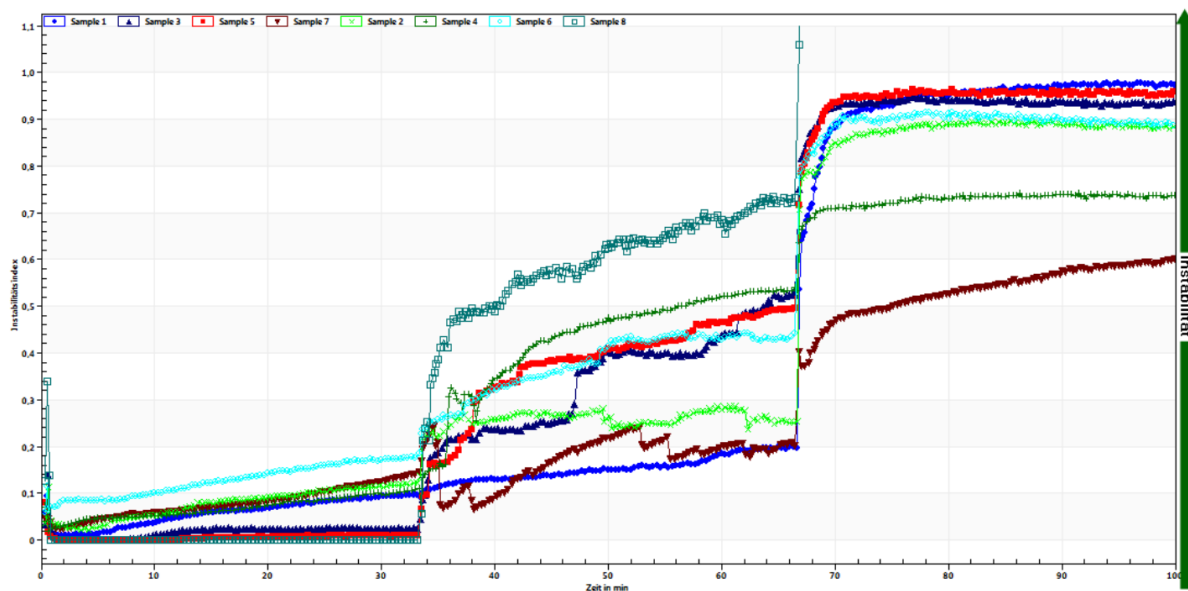


Figure 10: Instability Index over time

The stability of fully molten SAT samples was assessed using the instability index calculated by the LumiSizer software. The instability index is a dimensionless parameter derived from temporal changes in optical transmission profiles and is used to quantify structural inhomogeneities developing within the sample during centrifugation. (LUM GmbH, n.d.; Van Brakel & Modry, 2017)

Figure 10 shows the instability index as a function of time for eight molten SAT samples subjected to a stepwise centrifugal program. (Van Brakel & Modry, 2017) At the beginning of the measurement, all samples exhibit low instability index values close to zero, indicating a largely homogeneous molten state. During the first measurement interval, a gradual increase in the instability index is observed for all samples.

At approximately 35 min, a pronounced stepwise increase in the instability index occurs simultaneously for all samples. A second, more distinct increase is observed at around 65–70 min. Both step changes coincide with programmed increases in centrifugal acceleration, at first from 1000rpm to 2000rpm and then from 2000 to 4000rpm. After the second step, most samples reach a plateau at elevated instability index values.

Despite the common response to the centrifugal program, differences in the magnitude and progression of the instability index are evident between individual samples. Some samples show a steep increase immediately after the acceleration steps, while others exhibit a more gradual rise. No abrupt spikes or oscillations in the instability index were observed throughout the experiment. The detailed evaluation documentation of the LumiSizer can be seen in the digital Appendix 9B.4.

Sample 8

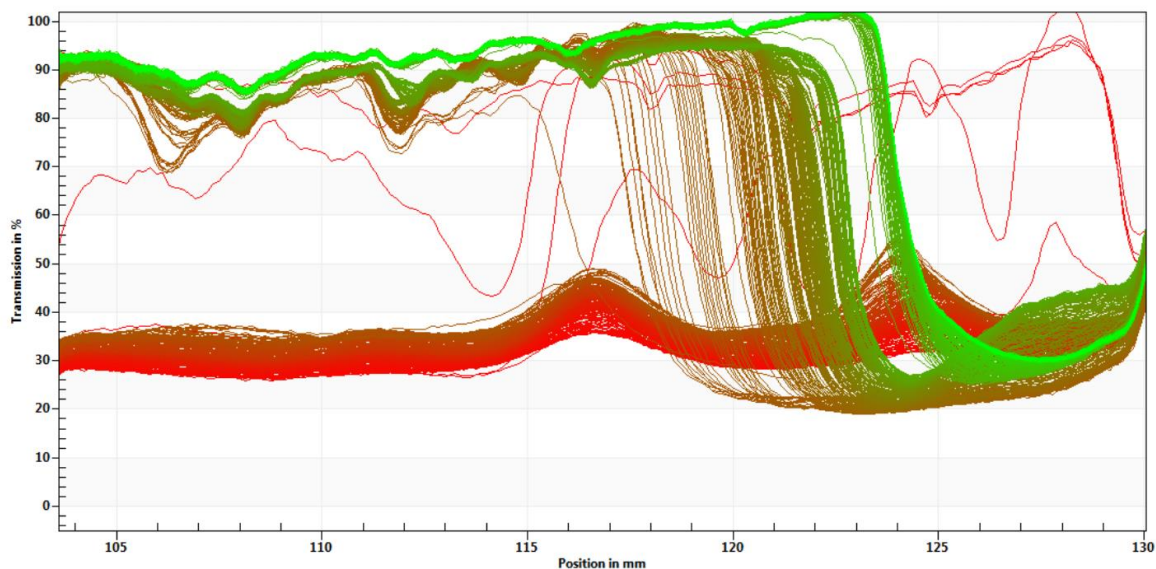


Figure 11: Radial Transmission Profiles

Figure 11 shows the evolution of the radial transmission profiles of Sample 8 measured with the LumiSizer. The profiles represent optical transmission as a function of radial position, with the green curves corresponding to the initial state of the measurement and the red curves corresponding to the final state after completion of the centrifugal program. (LUM GmbH, n.d.)

At the start of the experiment, Sample 8 exhibits a generally high transmission level over most of the radial domain. A pronounced reduction in transmission is already visible at larger radial positions in the initial profiles.

During the centrifugal program, the position of the transmission dip remains largely unchanged, while its magnitude increases toward the end of the measurement. The transmission profiles evolve smoothly over time, without abrupt drops, discontinuities, or propagating features.

Overall, the radial transmission profiles show a predominantly homogeneous transmission behavior over the majority of the sample length with a persistent localized region of reduced transmission at larger radial positions throughout the experiment. (Van Brakel & Modry, 2017)

4.3 EasyMax – Experiment 4 and 5

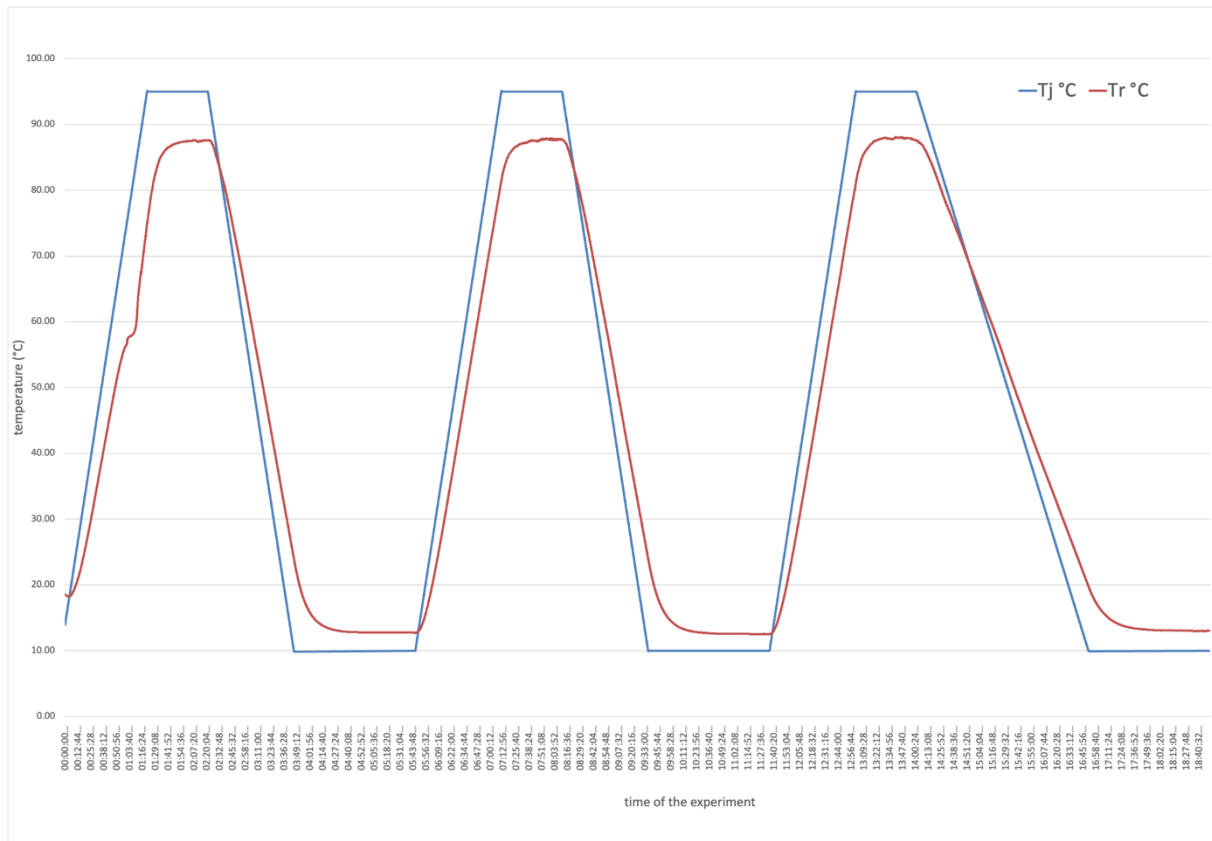


Figure 12: Temperature over Time Profile of Experiment 4

Experiment 4 – Cyclic Thermal Loading with Reduced Dynamic Response

Figure 12 presents the temperature evolution of the jacket temperature T_j and the recorded sample temperature T_r during the first experiment. (METTLER TOLEDO, n.d.-c) The system was subjected to three identical heating–cooling cycles, with T_j following a trapezoidal temperature profile between approximately 10 °C and 95 °C.

The measured temperature T_r follows the imposed T_j profile qualitatively but exhibits a clear temporal delay during both heating and cooling phases. During the heating ramps, T_r increases smoothly and asymptotically approaches a maximum temperature of approximately 87–88 °C, remaining consistently below the jacket temperature. No overshoot beyond the target temperature is observed. During the isothermal holding phases at high temperature, T_r stabilizes at a nearly constant value, indicating that thermal equilibrium is approached but not fully reached within the holding time. (METTLER TOLEDO, n.d.-c)

During the cooling phases, T_r decreases continuously with a noticeably slower rate compared to T_j . At the lower temperature plateau, T_r stabilizes at approximately 12–13 °C, again remaining slightly above the jacket temperature minimum. Across all three cycles, the temperature profiles are highly reproducible, with negligible cycle-to-cycle variation.

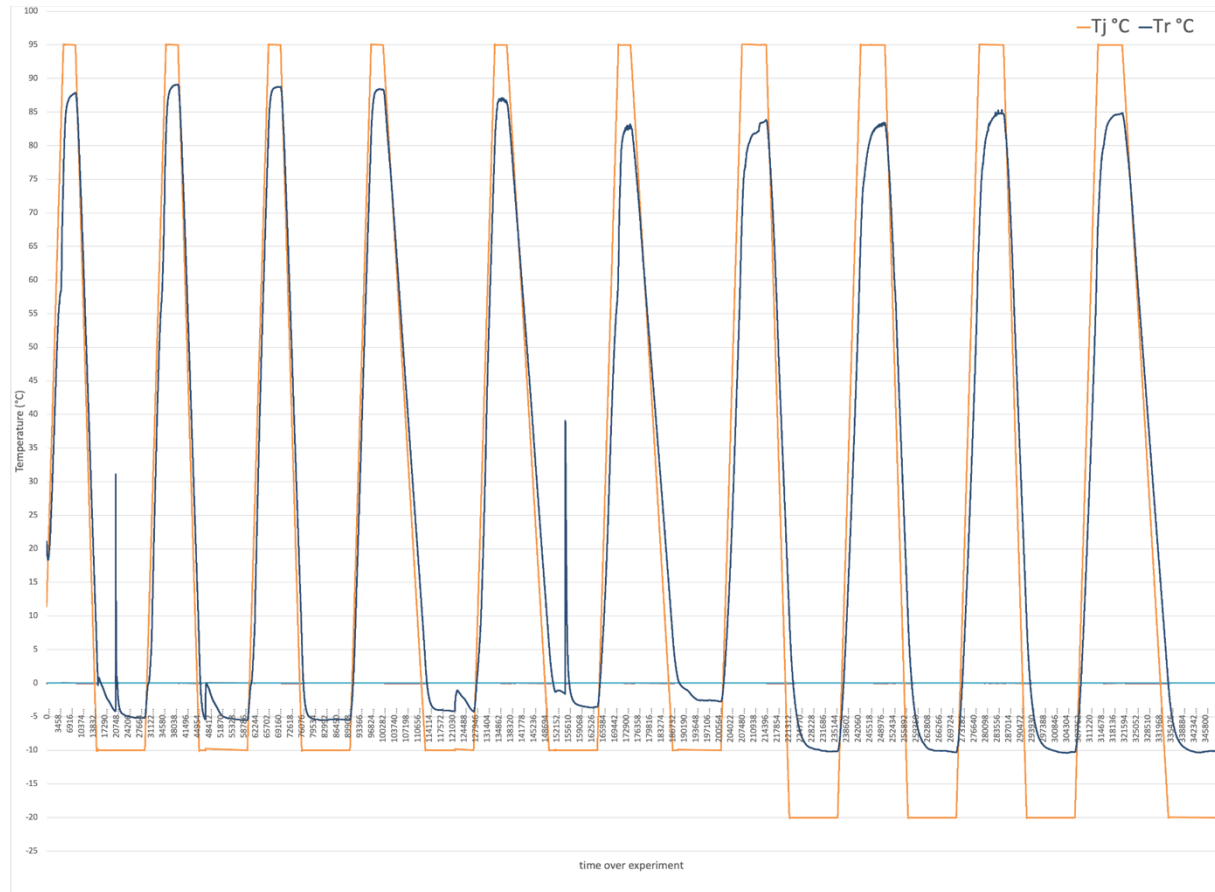


Figure 13: Temperature over time of Experiment 5

Experiment 5 – High-Frequency Thermal Cycling with Supercooling and Crystallization Trigger Assessment

Figure 13 shows the temperature evolution of the jacket temperature T_j and the measured sample temperature T_r during the second experiment. In comparison to Experiment 4, this experiment comprises a significantly larger number of thermal cycles and extends the lower jacket temperature limit to approximately -20 °C, while maintaining an upper limit of approximately 95 °C. The lower temperature was deliberately selected to assess whether sufficiently deep cooling is capable of triggering the crystallization of sodium acetate trihydrate. (Beaupère et al., 2020)

The jacket temperature T_j follows a repetitive trapezoidal profile with steep heating ramps, short high-temperature holding phases, and rapid cooling to sub-zero temperatures.

The sample temperature T_r follows the imposed temperature profile qualitatively but exhibits a pronounced temporal delay and damping relative to T_j .

During heating, T_r increases rapidly and reaches peak temperatures between approximately 82 °C and 88 °C, remaining consistently below T_j . Thermal equilibrium is not reached within the short holding phases. This behavior remains stable and repeatable across all cycles.

During cooling, T_j decreases to approximately -20 °C, while T_r stabilizes at higher temperatures, typically between -5 °C and -10 °C. At several low-temperature plateaus, distinct short-duration temperature spikes are observed. (Beaupère et al., 2020) Distinct short-duration temperature spikes were observed exclusively in the negative temperature range and coincide with the onset of crystallization in the sodium acetate trihydrate sample. The spikes are abruptly terminated when the programmed temperature profile of T_j transitions from cooling to reheating.

5 Discussion of Results

The experimental results, considered collectively across the applied laboratory methods, reveal a coherent set of interdependencies governing the supercooling, crystallization behavior, and stability of sodium acetate trihydrate under controlled conditions. These findings demonstrate that achieving controlled and reproducible crystallization in phase change materials requires more than isolated thermal control. It necessitates a coordinated consideration of material properties, water content, mechanical loading, and temperature program design. The combined analysis of water content determination, stability assessment, and thermal cycling enables the identification of critical parameters that govern crystallization behavior. This chapter discusses these implications and derives corresponding conclusions for the design and feasibility of future microgravity experiments.

5.1 Experiment 1 and 2

The significant discrepancy between the results obtained from the Karl Fischer titrator and the halogen moisture analyzer has important implications for subsequent sample handling. (METTLER TOLEDO, n.d.-a; METTLER TOLEDO, n.d.-b) As the experimental requirements specify that all experiments must be conducted with SAT at its standard water content, without intentional addition or removal of water, a reliable determination of the moisture content is essential. The repeated Karl Fischer measurements showed consistent results, indicating higher reliability for this method. (METTLER TOLEDO, n.d.-a) Consequently, the deviation between the two methods was attributed to the limited accuracy of the halogen moisture analyzer for this application. (METTLER TOLEDO, n.d.-b; METTLER TOLEDO, 2025) For all subsequent experiments, the Karl Fischer Ti-Touch titrator was therefore used as the reference method. Based on these results, water was added to the SAT samples to adjust the moisture content to the standard value of 39.7%.

5.2 Experiment 3

The evolution of the instability index reflects the response of molten sodium acetate trihydrate to increasing centrifugal stress. (Van Baren, 2017) The low initial values confirm that the samples were largely homogeneous after melting and prior to centrifugation. The gradual increase observed during the first measurement phase can be attributed to the formation of transient density gradients as the molten SAT redistributes under the applied centrifugal field.

The stepwise increases in the instability index correspond directly to increases in centrifugal acceleration, demonstrating that the instability index is strongly governed by external mechanical forcing rather than by spontaneous material transformations. (Van Baren, 2017) Higher centrifugal forces enhance density-driven separation within the liquid phase, leading to stronger optical gradients and consequently higher instability index values. (Van Baren, 2017)

Importantly, the increase in the instability index does not indicate crystallization or phase separation in the classical sense. The absence of abrupt drops, sharp peaks, or erratic behavior suggests that no rapid solidification or sedimentation processes occurred during the measurement. Instead, the observed plateaus at higher instability index values indicate a stable redistribution of the molten SAT under sustained centrifugal conditions.

Sample-to-sample variations in the instability index trends likely originate from minor differences in water content, residual undissolved particles, or trapped gas bubbles introduced during melting and sample preparation. These results highlight the sensitivity of molten SAT to preparation history and underline the necessity of consistent handling procedures. Overall, the instability index analysis confirms that molten SAT remains physically stable under the applied centrifugal stresses and is suitable for subsequent investigations focusing on supercooling and controlled crystallization behavior.

Sample 8

The radial transmission profiles of Sample 8 provide important insight into the local stability and microstructural behavior of molten sodium acetate trihydrate under centrifugal acceleration. The persistence of a transmission dip at larger radial positions from the start of the experiment indicates that this feature is not induced by centrifugation but rather originates from initial sample conditions.

The most plausible primary explanation for this behavior is the influence of optical boundary effects. (Van Baren, 2017) Near the cuvette wall, changes in optical path length, refraction, and meniscus curvature lead to increased scattering which reduces the measured transmission even in a fully molten and homogeneous sample. The fact that the radial position of the dip remains nearly constant throughout the experiment supports this interpretation, as geometric and optical boundary conditions are invariant during centrifugation. The unchanged radial position of the transmission dip suggests an amplification of pre-existing density or concentration gradients rather than the formation of new structural features during centrifugation.

However, given the known supercooling characteristics of sodium acetate trihydrate, a secondary contribution from localized partial solidification cannot be excluded. (Ma et al., 2017; Machida et al., 2017)

SAT is known to allow local nucleation without immediate propagation of crystallization through the entire sample. (Ma et al., 2017) A thin crystal-rich region forming near the sample boundary could therefore persist without triggering bulk solidification, particularly if the released latent heat is dissipated locally. Such a localized solid phase would increase light scattering and may contribute to the observed reduction in transmission.

Importantly, the absence of abrupt transmission losses, instability oscillations, or propagating phase boundaries indicates that Sample 8 did not undergo macroscopic crystallization during the experiment. This interpretation is consistent with the smooth evolution of the transmission profiles and the lack of sudden changes typically associated with nucleation events. The centrifugal field thus appears to enhance existing gradients rather than initiate a phase transition.

Overall, the combined results suggest that Sample 8 remained predominantly molten and structurally stable throughout the measurement. The observed transmission dip reflects either persistent optical boundary effects or, at most, a limited and non-propagating solid fraction. These findings underline the importance of careful sample preparation and controlled boundary conditions when interpreting spatially resolved optical measurements of supercooled phase change materials. This behavior confirms that the sample remained suitable for subsequent investigations focusing on controlled nucleation and crystallization behavior. At the same time, they confirm that the LumiSizer can detect subtle local heterogeneities without necessarily indicating bulk instability or crystallization.

5.3 Experiment 4 and 5

The results of Experiment 5 confirm that the applied lower temperature boundary condition is sufficient to induce supercooling in sodium acetate trihydrate. (Machida et al., 2017) The extension of the cooling range to $-20\text{ }^{\circ}\text{C}$ was intentionally chosen to investigate whether deep undercooling alone can trigger crystallization in the sample.

The observed temperature spikes represent clear signatures of supercooling; however, no sustained temperature rise associated with full crystallization is observed. (Machida et al., 2017; Ma et al., 2017) This indicates that while the imposed low temperature is sufficient to initiate supercooling, it is not sufficient to reliably trigger complete crystallization under the given experimental conditions.

The supercooled state is further interrupted by the programmed increase in T_j . As the jacket temperature begins to rise, the thermal driving force for continued undercooling is removed, effectively cutting off the supercooling process before crystallization can fully develop. As a result, no prolonged exothermic plateau or significant latent heat release is detected in Tr .

In contrast, Experiment 1 does not reach temperatures low enough to initiate supercooling and therefore shows no comparable thermal features. The comparison between the two experiments demonstrates that while deep cooling is a necessary condition for supercooling in SAT, it is not, on its own, a sufficient condition to ensure controlled crystallization within short cycle durations. (Machida et al., 2017)

Overall, these findings highlight the critical role of minimum temperature and temperature program design when investigating supercooling and crystallization behavior in sodium acetate trihydrate. They further indicate that additional triggering mechanisms or extended low-temperature dwell times may be required to achieve reproducible crystallization in subsequent experiments.

6 Conclusion

This thesis investigated the crystallization behavior of selected inorganic phase change materials under controlled laboratory conditions with the explicit objective of supporting the design and parameter definition of a future microgravity experiment on a MASER sounding rocket. The focus was placed on sodium acetate trihydrate (SAT) and calcium chloride hexahydrate (CCH) with particular attention to supercooling behavior, crystallization controllability, and experimental feasibility under space-relevant constraints.

A structured decision process based on thermophysical properties, operational robustness, and system-level requirements demonstrated that SAT is better suited than CCH for controlled crystallization experiments in microgravity. (Ma et al., 2017; Wang et al., 2019) While CCH offers higher thermal conductivity and faster crystallization kinetics, its tendency toward incongruent melting, spontaneous nucleation, and corrosive behavior introduces significant risks for small-scale rocket payloads. In contrast, SAT exhibits congruent melting, high cycle stability, safe handling characteristics, and, most importantly, a pronounced and reproducible supercooled state that enables controlled, on-demand nucleation. (Ma et al., 2017)

The experimental investigations confirmed the critical importance of accurate water content determination for SAT. A significant discrepancy between Karl Fischer titration and halogen moisture analysis was observed, with the Karl Fischer method proving to be substantially more reliable for salt hydrate characterization. Ensuring the correct hydration state was shown to be a prerequisite for reproducible thermal behavior and meaningful interpretation of subsequent experiments.

Stability analysis using the LumiSizer demonstrated that fully molten SAT remains structurally stable under elevated centrifugal accelerations. (Van Baren, 2017) The observed increase in instability index was directly correlated with externally applied centrifugal forces rather than intrinsic material instability or crystallization. This confirms that molten SAT can tolerate significant mechanical loading without undergoing phase separation or unintended solidification, supporting its suitability for launch and ascent conditions.

Thermal cycling experiments performed with the EasyMax system revealed that deep cooling to sub-zero temperatures is sufficient to induce supercooling in SAT but not sufficient to reliably trigger complete crystallization within short cycle durations. The observed temperature spikes at negative temperatures were identified as signatures of incipient supercooling that were repeatedly interrupted by reheating phases, preventing sustained latent heat release. These findings highlight that crystallization of SAT cannot be reliably achieved by temperature control

alone and that additional triggering mechanisms or extended low-temperature dwell times are required.

Overall, this thesis demonstrates that a supercooling-dominated operational strategy using sodium acetate trihydrate is the most suitable approach for investigating crystallization under microgravity conditions. (Machida et al., 2017; Ma et al., 2017) The experimental results generated provide essential boundary conditions, limitations, and design inputs for a future sounding rocket experiment, thereby significantly reducing technical risk and uncertainty.

7 Recommendations and Outlook

The findings of this study provide a set of practical and forward-looking recommendations for the design and implementation of future phase change material experiments under microgravity conditions. Building on the experimental results and their interpretation, this chapter translates the identified limitations and influencing factors into concrete guidance for experiment design, operational strategy, and risk reduction. In addition, remaining challenges and open questions are outlined to support further development and validation of controlled crystallization concepts for sounding rocket applications.

7.1 Implications of Laboratory Results for Microgravity Experiments

The laboratory results obtained in this study have direct implications for the design of crystallization experiments under microgravity conditions. First, the strong sensitivity of SAT to water content variations underscores the necessity of precise sample preparation and verification prior to flight. Karl Fischer titration should be considered mandatory for payload qualification to ensure reproducible thermal behavior. (METTLER TOLEDO, n.d.-a)

Second, the stability of molten SAT under centrifugal loading indicates that mechanical stresses during launch and ascent are unlikely to induce premature crystallization or phase separation, provided that thermal conditions are appropriately controlled. (Van Baren, 2017) This supports the feasibility of transporting SAT in a molten or supercooled state to the microgravity phase.

Third, the EasyMax experiments demonstrate that supercooling alone does not guarantee crystallization within short experimental windows. Consequently, crystallization in microgravity should not rely solely on thermal boundary conditions but must incorporate an active and well-defined triggering mechanism. (Machida et al., 2017)

7.2 Future Experiment Setup on MASER Sounding Rocket

For future MASER experiments, a supercooling-based experimental concept using sodium acetate trihydrate is strongly recommended. The following design elements should be prioritized:

- **Active crystallization triggering**, such as mechanical seeding, localized thermal pulses, or controlled nucleation surfaces, to ensure reproducible crystallization during the microgravity phase.
- **Extended low-temperature dwell times** prior to triggering, enabling sufficient undercooling without premature reheating.

- **Redundant temperature sensing** within the PCM sample to clearly distinguish between supercooling onset, partial crystallization, and full solidification.
- **Minimized thermal coupling to the payload structure**, reducing unintended heat inflow that could suppress crystallization.

Furthermore, sample geometry and volume should be carefully optimized to balance observable crystallization fronts with the limited thermal mass and power constraints of sounding rocket payloads.

7.3 Design Constraints and Open Challenges

Despite the promising results, several open challenges remain. The short duration of microgravity limits the time available for crystallization and heat release, placing strict demands on triggering reliability and timing accuracy. Additionally, vibration, residual accelerations, and thermal gradients during flight may influence nucleation behavior in ways that cannot be fully replicated on Earth.

Future work should therefore include drop-tower or parabolic-flight experiments to bridge the gap between laboratory and rocket conditions. (Swedish Space Corporation, 2014) Numerical modeling of heat transfer and crystallization kinetics under reduced gravity could further support payload optimization.

In conclusion, this thesis provides a robust experimental and conceptual foundation for future microgravity investigations of PCM crystallization. By demonstrating the feasibility and limitations of supercooling-controlled operation with sodium acetate trihydrate, it contributes directly to the advancement of reliable latent heat thermal energy storage systems for space applications.

8 References

Beaupère, N., Soupremanien, U., & Zalewski, L. (2020).

Experimental measurements of the residual solidification duration of a supercooled sodium acetate trihydrate. *International Journal of Thermal Sciences*, *158*, 106544.

<https://doi.org/10.1016/j.ijthermalsci.2020.106544>

Chen, W., Chen, L., Li, L., Dong, C., & Zhang, L. (2023).

Electrically triggered nucleation of supercooled sodium acetate trihydrate phase change composites. *Chemical Engineering Journal*, *456*, 141131.

<https://doi.org/10.1016/j.cej.2022.141131>

Dong, C., Qi, R., Yu, H., & Zhang, L. (2022).

Electrically controlled crystallization of supercooled sodium acetate trihydrate solution. *Energy and Buildings*, *260*, 111948.

<https://doi.org/10.1016/j.enbuild.2022.111948>

Englmair, G., Moser, C., Schranzhofer, H., Fan, J., & Furbo, S. (2019).

A solar combi-system utilizing stable supercooling of sodium acetate trihydrate for heat storage: Numerical performance investigation. *Applied Energy*, *242*, 1108–1120.

<https://doi.org/10.1016/j.apenergy.2019.03.125>

Halogen Moisture Analyzer. (n.d.).

How a halogen moisture analyzer works.

<https://www.halogenmoistureanalyzer.com/resources/how-halogen-moisture-analyzer-works>

Kong, W., Dannemand, M., Brinkø Berg, J., Fan, J., Englmair, G., Dragsted, J., & Furbo, S. (2019).

Experimental investigations on phase separation for different heights of sodium acetate water mixtures under different conditions. *Applied Thermal Engineering*, *148*, 796–805.

<https://doi.org/10.1016/j.applthermaleng.2018.10.017>

Krämer, S. (2025).

SubOrbital Express / SIX 5-M17 interface and environment description – Shared module – Active system experiment.

LUM GmbH. (n.d.).

LUMiSizer® analytical centrifuge: Product information.

<https://www.lum-gmbh.com/products/lumisizer/>

Ma, Z., Bao, H., & Roskilly, A. P. (2017).

Study on solidification process of sodium acetate trihydrate for seasonal solar thermal energy storage. *Solar Energy Materials and Solar Cells*, 172, 99–107.

<https://doi.org/10.1016/j.solmat.2017.07.024>

Machida, H., Sugahara, T., & Hirasawa, I. (2017).

Relationship between supercooling stability and solution structure in sodium acetate aqueous solution. *Journal of Crystal Growth*, 475, 295–299.

<https://doi.org/10.1016/j.jcrysgr.2017.07.006>

MASER Program. (2014).

MASER user manual change record.

<https://www.sscspace.com>

Metrohm. (n.d.).

Karl Fischer titration: Theory, principles, and applications.

<https://www.metrohm.com/en/applications/chemical-analysis/titration/karl-fischer-titration>

METTLER TOLEDO. (n.d.).

Guide to moisture analysis.

<https://www.mt.com/us/en/home/library/guides/laboratory-weighing/guide-to-moisture-analysis.html>

METTLER TOLEDO. (2025).

HX204 halogen moisture analyzer: Datasheet (30019639D) METTLER TOLEDO Group.

Montgomery, D. C. (2017).

Design and analysis of experiments (9th ed.). John Wiley & Sons.

Shamseddine, I., Pennec, F., Biwole, P. H., & Fardoun, F. (2022).

Supercooling of phase change materials: A review. *Renewable and Sustainable Energy Reviews*, *158*, 112172.

<https://doi.org/10.1016/j.rser.2022.112172>

Sharma, A., Tyagi, V. V., Chen, C. R., & Buddhi, D. (2009).

Review on thermal energy storage with phase change materials and applications. *Renewable and Sustainable Energy Reviews*, *13*(2), 318–345.

<https://doi.org/10.1016/j.rser.2007.10.005>

Skoog, D. A., West, D. M., Holler, F. J., & Crouch, S. R. (2014).

Fundamentals of analytical chemistry (9th ed.). Cengage Learning.

van Baren, J. (2017).

Test my product using sine or random? *Vibroengineering Procedia*, *16*, 102–107.

<https://doi.org/10.21595/vp.2017.19354>

Van Brakel, J., & Modry, S. (2017).

Analytical centrifugation for the characterization of dispersions. *Particle & Particle Systems Characterization*, *34*(6), 1600429.

<https://doi.org/10.1002/ppsc.201600429>

Wang, Y., Yu, K., Peng, H., & Ling, X. (2019).

Preparation and thermal properties of sodium acetate trihydrate as a novel phase change material for energy storage. *Energy*, *167*, 269–274.

<https://doi.org/10.1016/j.energy.2018.10.164>

Worlitschek, J., Stamatiou, A., Ravotti, R., Hochuli, A., & Wüest, S. (n.d.).

TripleF – Freeze, flow, and form: Microgravity effects on the solidification of phase change materials.

9 Appendix

A	Declaration of the Use of AI-based Tools	52
B	Table of Contents of Digital Appendix.....	53
B.1	Full Experimental Matrix.xls	53
B.2	Proposal_TripleF (Source_Worlitschek et al_nd).pdf.....	53
B.3	Experiment 1_Methrom 915_doku.pdf.....	53
B.4	Experiment 3_LumiSizer_full doku.pdf.....	53
B.5	Experiment 3_Sample 8_LumiSizer_doku sample 8.pdf.....	53
B.6	Experiment 4_EasyMax	53
B.7	Experiment 5_EasyMax	53
B.8	HalogenDryer_Experiments	53
B.9	EasyMax_Other Experiments.....	53
B.10	LumiSizer_Other Experiments.....	53
B.11	Other Experiments.....	53

A Declaration of the Use of AI-based Tools

AI based tool	Use case	Scope
Chat-GPT 5.1/5.2	Grammar correction, expression standardization, proofreading	Entire work
Chat-GPT 5.1/5.2	Self-understanding of literature	Introduction, Literature review
Chat-GPT 5.1/5.2	Create first drafts of continuous text based on own notes	Entire Work
DeepL Translate	Translation German English	Entire work
Mendeley	Structure and creation of references	Chapter 8

B Table of Contents of Digital Appendix

B.1 Full Experimental Matrix.xls

B.2 Proposal_TripleF (Source_Worlitschek et al_nd).pdf

B.3 Experiment 1_Methrom 915_doku.pdf

B.4 Experiment 3_LumiSizer_full doku.pdf

B.5 Experiment 3_Sample 8_LumiSizer_doku sample 8.pdf

B.6 Experiment 4_EasyMax

B.7 Experiment 5_EasyMax

B.8 HalogenDryer_Experiments

B.9 EasyMax_Other Experiments

B.10 LumiSizer_Other Experiments

B.11 Other Experiments